0013-4686(94)E0085-E

ELECTROLESS AMORPHOUS ALLOY ELECTRODES—THE FORMATION AND PROPERTIES OF HYDROUS OXIDE COATINGS IN ALKALINE SOLUTION

T. Kessler,* J. J. Podestá,† R. C. V. Piatti,† W. E. Triaca† and A. J. Arvia†

* Facultad de Ingeniería, Universidad Nacional del Centro de la Provincia de Buenos Aires, Casilla de Correo 12, 7400 Olavarría, Argentina
† Instituto de Investigaciones Fisicoquímicas Teóricas y Aplicadas (INIFTA), Facultad de Ciencias Exactas, Universidad Nacional de La Plata, Sucursal 4, Casilla de Correo 16, 1900 La Plata, Argentina

Abstract—Amorphous alloys ($Co_{94.6}P_{5.4}$ and $Co_{71.6}Ni_{18.3}P_{10.1}$) were prepared by the electroless technique. Oxide coated amorphous alloys were produced by applying a cyclic potential routine to the amorphous alloys immersed in alkaline solution at 30°C. Oxide coatings were characterized by electrochemical techniques and ir spectroscopy. The electrocatalytic activity of oxide coated amorphous alloy electrodes was tested for the oxygen evolution reaction in alkaline solution at 30°C. The high electrocatalytic activity of these electrodes is explained through the development of a porous hydrous oxide film with a spinel-type structure.

1. INTRODUCTION

Amorphous alloys are promising low cost electrocatalysts for water electrolysis in alkaline solutions[1–3]. Among several methods, electroless deposition appears as a relatively easy way for tailoring desired amorphous alloy compositions on either conductor or insulator materials[4–6].

Hydrous oxide coatings of controlled thicknesses can be easily grown by applying cyclic potential routines to either metals or amorphous alloys immersed in aqueous solution[7–12]. For Co–Ni amorphous alloys, hydrous oxide films which are precursors of spinel-structures have been obtained[12]. This type of oxide coated electrodes exhibits a high electrocatalytic activity towards the oxygen evolution reaction (*oer*) in alkaline solution[13].

This work describes the optimal conditions for the preparation of hydrous oxide coatings on electroless-prepared $Co_{94.6}P_{5.4}$ and $Co_{71.6}Ni_{18.3}P_{10.1}$ electrodes by applying a square wave potential routine (SWPR) in alkaline solution, and their characterization.

2. EXPERIMENTAL

The working electrodes (*we*) consisted of an amorphous alloy of about $20\,\mu m$ in thickness which was electroless-deposited on standard Al_2O_3 wafers as described elsewhere[6]. Amorphous alloy compositions in atg% were represented by the following stoichiometric formula, $Co_{94.6}P_{5.4}$ and $Co_{71.6}Ni_{18.3}P_{10.1}$[6].

Runs were made in a conventional three-electrode glass cell in 1 M NaOH at 30°C under N_2 saturation. A large Pt foil counter electrode (*ca.* $10\,cm^2$) and a reversible hydrogen reference electrode (*rhe*) in the same solution were used.

The *we* were potential cycled at $0.1\,V\,s^{-1}$ between 0.30 and 1.55 V for 10 min and then subjected to the SWPR treatment to produce an oxide coating. The SWPR parameters covered the following ranges: $0 \leqslant E_u \leqslant 2\,V$; $-2 \leqslant E_1 \leqslant 0\,V$; $0.025 \leqslant f \leqslant 5\,kHz$; $5 \leqslant t \leqslant 120\,s$, where E_u and E_1 are the anodic and cathodic switching potentials, respectively; f and t are the frequency and the duration of the SWPR treatment, respectively. SWPR treatments under the above mentioned conditions provided amorphous alloy electrode surfaces without traces of Pt, at least as revealed by XPS analysis[12]. It should be noted that for the optimal value of f, *ie* $f = 0.1\,kHz$, in alkaline solutions, no Pt electrodissolution could be detected, in contrast to results obtained in acid solutions at lower values of f[14, 15]. Occasionally, the oxide coated *we* were further treated at 380°C under N_2 atmosphere. Then, three types of *we* were used, namely, untreated (type I), oxide coated (type II) and thermally treated oxide coated (type III) electrodes.

The relative increase in the amount of oxide accumulated on the *we* was evaluated through the ratio, $R = Q_a/Q_b$, where Q_b and Q_a are the overall voltammetric charge obtained from the stabilized voltammogram at $0.1\,V\,s^{-1}$, before and after the above mentioned treatments, respectively.

Quasi-steady-state polarization curves for the *oer* were determined at $10^{-4}\,V\,s^{-1}$. The current density (j) was referred to the *we* geometric area ($1\,cm^2$).

Electrochemical data were complemented with *ir* spectra of powdered metal oxide coatings.

3. RESULTS

Stabilized voltammograms run at $0.1 \, Vs^{-1}$ between 0.30 and 1.55 V for Co–P amorphous alloys before and after the SWPR treatment ($E_u = 1.6 \, V$, $E_l = -1.6 \, V$, $f = 0.1 \, kHz$; $t = 1 \, min$) (Fig. 1a) show two main pairs of current peaks located at about 1.0 and 1.5 V which resemble those found for poly-crystalline (*pc*) Co and electroless-prepared Co electrodes in alkaline solution. These peaks were assigned to the $Co(OH)_2/Co_3O_4$ and the $Co(OH)_2/CoOOH$ redox reactions[16–19]. A slight voltammetric charge increase yielding $R = 4$ can be observed in going from type I to type II Co–P *we* (Fig. 1a).

For Co–Ni–P amorphous alloys, the voltammograms run at $0.1 \, Vs^{-1}$ between 0.30 and 1.55 V for type I *we* and type II *we* are depicted in Fig. 1b. The voltammogram of type I *we* shows two anodic peaks located at about 1.05 and 1.35 V and a cathodic peak at 1.35 V, which were assigned to the Ni(II)/Ni(III) and Co(III)/Co(IV) redox reactions[20–27]. Otherwise, the voltammogram of type II *we* prepared by SWPR treatment ($E_u = 1.0 \, V$, $E_l = -1.7 \, V$, $f = 0.1 \, kHz$, $t = 1 \, min$), shows only one pair of current peaks which resembles that reported for either Co–Ni and Co-spinels[20, 23, 26, 27] or galvanostatically deposited Co–Ni–P alloys[28, 29]. On the other hand, the increase in voltammetric charge for the type II Co–Ni–P amorphous alloy ($R = 24$) (Fig. 1b) is greater than that for the type II Co–P amorphous alloy (Fig. 1a).

SWPR parameters were systematically changed in order to achieve the largest value of R. For Co–P amorphous alloys, the optimal value $E_u = 1.6 \, V$ was approached by setting $f = 0.1 \, kHz$ and E_l exceeding the hydrogen evolution reaction (*her*) threshold potential (Fig. 2a). Correspondingly, by setting $E_u = 1.6 \, V$ and $f = 0.1 \, kHz$, the greatest value of R was attained for $E_l = -1.6 \, V$ (Fig. 2b). Likewise, by

Fig. 2. Dependence of R on E_u (a) and R on E_l (b) for Co–P and Co–Ni–P electrodes after 1 min SWPR treatment at $f = 0.1 \, kHz$: (□) Co–P alloy ($E_l = -1.0 \, V$); (○) Co–Ni–P alloy ($E_l = -1.0 \, V$); (■) Co–P alloy ($E_u = 1.6 \, V$); (●) Co–Ni–P alloy ($E_u = 1.0 \, V$). Data taken from voltammograms run at $0.1 \, Vs^{-1}$ in 1 M NaOH; 30°C.

setting $E_u = 1.6 \, V$ and $E_l = -1.6 \, V$, the optimal value $f = 0.1 \, kHz$ was found (Fig. 3). Analogously, for Co–Ni–P amorphous alloys the optimal SWPR parameters were $E_u = 1.0 \, V$, $E_l = -1.7 \, V$ and $f = 0.1 \, kHz$ (Figs 2 and 3).

Ir spectra of type I Co–P amorphous alloy powders show no absorption bands in the 4000–400 cm^{-1} range (Fig. 4a). Otherwise, *ir* spectra of air-dried powdered oxide coatings display a broad absorption band at *ca.* 580 cm^{-1} (Fig. 4b), whereas for thermally-treated powdered oxide coatings samples bands at 560 and 660 cm^{-1} (Fig. 4c and d), which are typical of chemically prepared Co_3O_4 spinel[30, 31], are observed. On the other hand, for type I Co–Ni–P amorphous alloy powders, feature-less *ir* spectra are recorded (Fig. 4a). The spectra of air-dried powdered metal oxide coatings show an absorption band at *ca.* 580 cm^{-1} (Fig. 4b), which is similar to that reported for both hydrous Ni and Co oxide layers produced on *pc* Ni and *pc* Co electrodes by the same procedure[10, 11]. *ir* spectra of thermally treated powdered oxide coatings exhibit absorption bands at 560 and 660 cm^{-1} (Fig. 4c and d), which can be assigned to a Co-spinel structure[30, 31] as the same spectrum can be obtained from a chemically prepared Co_3O_4 spinel (Fig. 4). It should be noted that the main absorption bands of chemically prepared $NiCo_2O_4$ spinel and
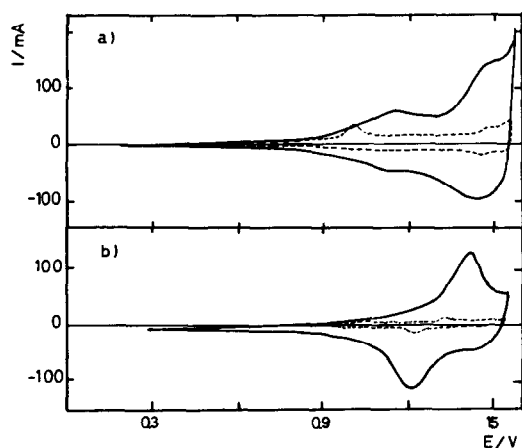

Fig. 1. Stabilized voltammograms at $0.1 \, Vs^{-1}$ for untreated (type I) (----) and oxide coated (type II) (——) Co–P (a) and Co–P–Ni (b) electrodes in 1 M NaOH; 30°C.
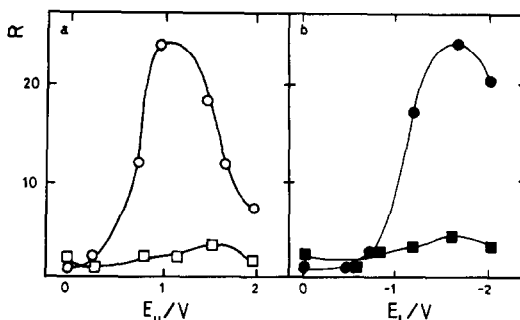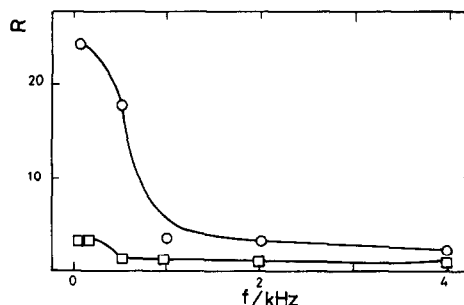

Fig. 3. Dependence of R on f for Co–P and Co–Ni–P electrodes after 1 min SWPR treatment: (□) Co–P alloy ($E_l = -1.6 \, V$; $E_u = 1.6 \, V$); (○) Co–Ni–P alloy ($E_l = -1.7 \, V$; $E_u = 1.0 \, V$). Data are taken from voltammograms run at $0.1 \, Vs^{-1}$ in 1 M NaOH; 30°C.
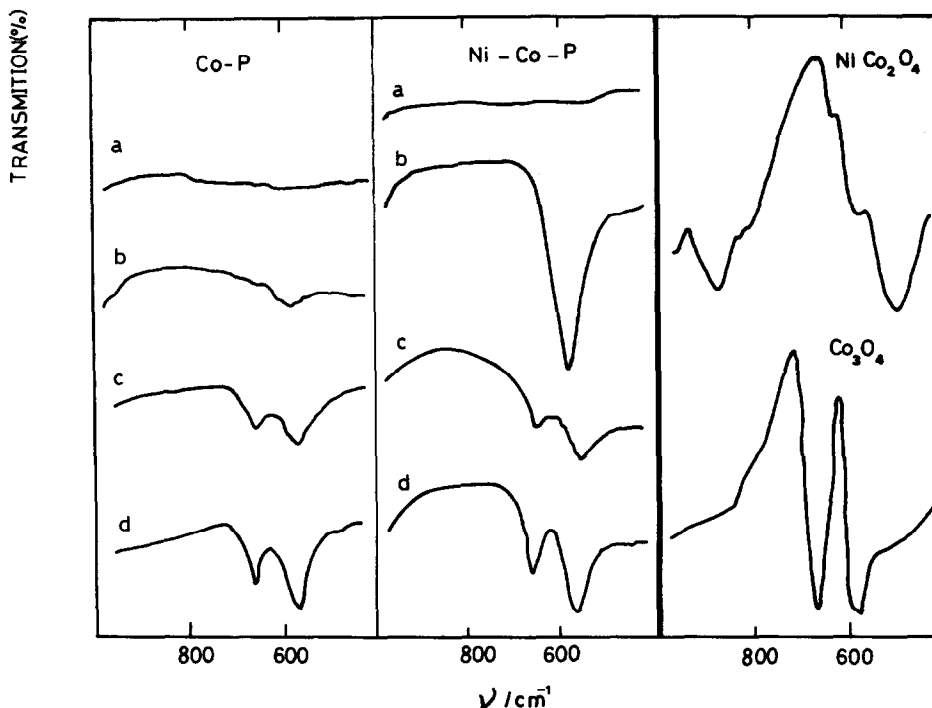
Fig. 4. *Ir* spectra of oxide powders resulting from untreated and SWPR treated Co–P and Co–Ni–P electrodes; chemically prepared Co–Ni and Co-spinels: (a) untreated samples; (b) air-dried powdered oxide coatings; (c) sample prepared as (b) and treated at 380°C for 2 h under N_2; (d) sample prepared as (b) and treated at 380°C for 21 h under N_2.

Ni oxide coatings produced by SWPR treatment[32], are expected at 480 and 560 cm^{-1} (Fig. 4) and at 420 and 650 cm^{-1}, respectively.

Polarization curves run at 10^{-4} V s^{-1} in the *oer* potential range were plotted as E vs. log j (Fig. 5). Tafel regions with slopes approaching 0.06 V decade^{-1} are obtained for both type I and type II Co–P *we*. Otherwise, similar current density values at constant potential are obtained from both type I and type II Co–P *we*.

For Co–Ni–P electrodes, the *oer* polarization curves fit Tafel lines with slopes of 0.04 V decade^{-1} and 0.06 V decade^{-1} for type I and type II *we*, respectively. Otherwise, the current density values at constant potential for both type I and type III Co–Ni–P *we* are also lower than those for type II *we*.
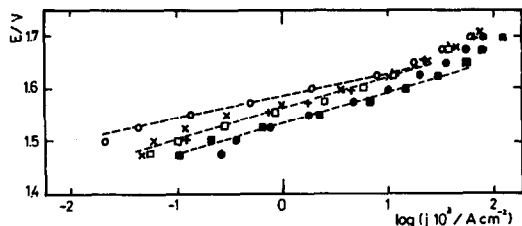

Fig. 5. Tafel plots derived from *oer* polarization curves for Co–P and Co–Ni–P electrodes in 1 M NaOH; 30°C. Untreated (type I) (□) Co–P and (○) Co–Ni–P alloys. Oxide coated (■) Co–P and (●) Co–Ni–P alloys. Oxide coated (+) Co–P and (×) Co–Ni–P alloys, after thermal treatment at 380°C during 21 h (type III).

4. DISCUSSION

4.1. Characteristics of oxide coatings

The comparison of *ir* spectra of SWPR treated amorphous alloys to those of chemically prepared Co_3O_4 and $NiCo_2O_4$ spinels demonstrates that a hydrous oxide coating which acts as a precursor of a Co-spinel structure is formed on electroless-deposited Co–P and Co–Ni–P amorphous alloys after the SWPR treatment, yielding a true spinel structure by thermal treatment at 380°C.

Likewise, after potential cycling, galvanostatically deposited Co–Ni–P amorphous alloys, exhibit the formation of only Co(OH), β-CoO(OH)$_2$ and α-Co phases as revealed by X-ray diffraction patterns, independently of the Co/Ni ratio in the alloy[28, 29].

The formation of spinel-type structures is also consistent with the first voltammograms resulting from type II Co–P and Co–Ni–P alloys which always show the same features as those obtained from SWPR treated *pc* Co[11]. Furthermore, the stabilized voltammograms for type III *we* exhibit a conjugated pair of peaks which resembles that reported for Co-spinels[19–21, 23, 27]. Therefore, for both Co–P and Co–Ni–P amorphous alloys it appears that the average composition of the oxide coating is dominated by Co oxides.

4.2. Optimal SWPR conditions for oxide coating formation

Type II *we* with the largest R values are produced by SWPR treatment with the following characteristics 1.6 V > E_u > 1.0 V; E_1 *ca.* —1.6 V and

$f = 0.1\,kHz$, the composition of these coatings being dominated by Co species. This result is consistent with the voltammetric behaviour of pc Ni and pc Co in alkaline solution[17, 33]. Thus pc Ni can be easily electro-oxidized to Ni(II) and Ni(III) oxi-hydroxide species within the E_u optimal range, although these species are hardly electroreduced to Ni(0) within the E_l optimal range. On the other hand, the voltammetric behaviour of pc Co in alkaline solution covering the E_l and E_u optimal range shows at least two reversible systems comprising only Co(0) and Co(II) oxidation states[17].

The electrochemical behaviour of pc Co and pc Ni under potential cycling conditions can explain the trend of Co electrode reactions to follow the potential routine yielding a $Co(OH)_2$ enriched layer for E_l values located in the her potential range. The low f value required for the $Co(OH)_2$ accumulation is presumably conditioned by the Co electrode kinetics[11, 12]. The formation of a relatively large amount of soluble Co^{2+} species and the precipitation and accumulation of $Co(OH)_2$ at E_l, are favoured at low f values.

4.3. Electrocatalytic influence of oxide coatings on oer

The oer Tafel slope (b_T) for type II Co–Ni–P we changes from 0.04 to $0.06\,V\,decade^{-1}$, ie to a typical Tafel slope for Co_3O_4 spinel in the same solution[21, 31].

This change in b_T can be due either to a change in the surface oxide layer composition or a change in the active sites characteristics caused by surface interactions. Otherwise, the change in b_T reported for crystalline Ni–Co alloys in alkaline solutions has also been explained by the different nature of surface oxides[21]. Thus, a $NiCo_2O_4$-spinel-like voltammetric behaviour is attained after potential cycling at $0.02\,V\,s^{-1}$ and, under these conditions, $b_T = 0.04\,V\,decade^{-1}$ has been reported, whereas preanodization at 1.8 V vs. rhe led to a Co_3O_4-type electrode for which $b_T = 0.06\,V\,decade^{-1}$[21].

As recently reported by Burke et al.[7, 9, 34], oxide layers produced on several metals by potential cycling improve the oer catalytic activity. This enhancement has been related to the hydrous structure of the oxide coatings produced by the potential routine treatment. Accordingly, hydrous oxide coatings are also produced by SWPR treatment of amorphous alloys. Furthermore, type II we can be described as spinel-type structures which exhibit a relatively large active surface area for the oer. In addition, type II we exhibit an oer catalytic activity higher than that of type III we. The lower catalytic activity of type III we can be attributed to the decrease in active surface area due to the dehydration caused by thermal treatment.

On the other hand, type II Co–P and Co–Ni–P we present similar current density values at constant potential despite the considerable difference in the corresponding values of R. Thus, it might be concluded that for both electrodes nearly the same active surface area is involved. The value of R is probably related to the total amount of oxide coating instead of the true active surface area for the oer. A comparable observation was made by Trasatti[19] about the meaning of roughness factor values as determined from voltammetry and capacitive current densities. Accordingly, the oer on type II we takes place predominantly on the external surface of oxide coatings, as earlier reported[35, 36].

5. CONCLUSIONS

Hydrous oxide films can be grown on electroless-prepared Co–P and Co–Ni–P amorphous alloys in alkaline solution by applying SWPR treatments under appropriate conditions.

For both amorphous alloys the hydrous oxide coatings are mainly formed by Co oxide species. These oxide coatings behave as precursors of Co-spinel structures. True spinel structures are produced by thermal treatment of hydrous oxide coated electrodes.

Both hydrous oxide coated amorphous alloys behave more active for the oer than the corresponding untreated and thermally treated oxide coated electrodes.

REFERENCES

1. G. Kreysa and B. Hakansson, J. electroanal. Chem. 201, 61 (1986).
2. A. Baiker, Faraday Discuss. Chem. Soc. 87, 239 (1989).
3. G. A. Tsirlina, O. A. Petrii and N. S. Kopylova, Elektrokhimiya 26, 1059 (1990).
4. F. Pearlstein, in Modern Electroplating (Edited by F. A. Lowenheim). John Wiley, New York (1974).
5. M. Schlesinger, in Electroless Deposition on Metals and Alloys, Proceedings, Vol. 88–12, p. 93. The Electrochemical Society, Pennington, New York (1988).
6. J. J. Podestá, R. C. V. Piatti, A. J. Arvia, P. Edkunge, K. Jüttner and G. Kreysa, Int. J. Hyd. Energy 17, 9 (1992).
7. L. D. Burke and O. J. Murphy, J. electroanal. Chem. 109, 373 (1980).
8. A. C. Chialvo, W. E. Triaca and A. J. Arvia, J. electroanal. Chem. 146, 93 (1983).
9. L. D. Burke and M. E. Lyons, in Modern Aspects of Electrochemistry, Vol. 18 (Edited by J. O'M. Bockris, B. E. Conway and R. E. White), p. 169. Plenum Press, New York (1986).
10. A. Visintin, A. C. Chialvo, W. E. Triaca and A. J. Arvia, J. electroanal. Chem. 225, 227 (1987).
11. T. Kessler, M. R. G. de Chialvo, A. Visintin, W. E. Triaca and A. J. Arvia, J. electroanal. Chem. 261, 315 (1989).
12. T. Kessler, W. E. Triaca and A. J. Arvia, J. appl. Electrochem. 23, 655 (1993).
13. T. Kessler, W. E. Triaca and A. J. Arvia, J. appl. Electrochem., 24, 310 (1994).
14. D. F. Untereker and S. Bruckenstein, J. electrochem. Soc. 121, 360 (1974).
15. C. L. Perdriel, W. E. Triaca and A. J. Arvia, J. electroanal. Chem. 205, 279 (1986).

16. W. K. Behl and J. E. Toni, *J. electroanal. Chem.* **31**, 63 (1971).
17. H. Gomez Meier, J. R. Vilche and A. J. Arvia, *J. electroanal. Chem.* **138**, 367 (1982).
18. T. R. Yayaraman, V. K. Venkatesan and H. V. K. Udupa, *Electrochim. Acta* **20**, 209 (1975).
19. R. Boggio, A. Carugati and S. Trasatti, *J. appl. Electrochem.* **17**, 828 (1987).
20. M. Hamdani, J. F. Koenig and P. Chartier, *J. appl. Electrochem.* **18**, 568 (1988).
21. J. Haenen, W. Visscher and E. Barendrecht, *Electrochim. Acta* **11**, 1541 (1966).
22. M. R. G. de Chialvo and A. C. Chialvo, *Electrochim. Acta* **36**, 963 (1991).
23. J. Haenen, W. Visscher and E. Barendrecht, *J. electroanal. Chem.* **208**, 273 (1986).
24. K. K. Lian and V. I. Birss, *J. electrochem. Soc.* **138**, 2877 (1991).
25. K. Lian, S. J. Thorpe and D. W. Kirk, *Electrochim. Acta* **37**, 2029 (1992).
26. P. Rasiyah, A. C. C. Tseung and D. B. Hibbert, *J. electrochem. Soc.* **129**, 1724 (1982).
27. D. B. Hibbert and Ch. R. Churchill, *J. Chem. Soc. Faraday Trans. I*, **80**, 1965 (1984).
28. A. Budniok and J. Kupka, *Electrochim. Acta* **34**, 871 (1989).
29. J. Kupka and A. Budniok, *J. appl. Electrochem.* **20**, 106 (1990).
30. J. Preudhomme and P. Tarte, *Spectrochim. Acta* **27A**, 1817 (1971).
31. M. R. Tarasevich and B. N. Efremov, in *Electrodes of Conductive Metallic Oxides* (Edited by S. Trasatti), Part A, p. 221. Elsevier, Amsterdam (1980).
32. A. Visintin, W. E. Triaca and A. J. Arvia, in preparation.
33. R. S. Schrebler Guzmán, J. R. Vilche and A. J. Arvia, *J. electrochem. Soc.* **125**, 1578 (1978).
34. L. D. Burke and E. J. M. O'Sullivan, *J. electroanal. Chem.* **117**, 155 (1981).
35. H. Wendt and V. Plzak, *Electrochim. Acta* **28**, 27 (1983).
36. S. P. Jiang and A. C. C. Tseung, *J. electrochem. Soc.* **138**, 1216 (1991).